

Anisotropic magnetoresistance with cubic anisotropy and weak ferromagnetism: A new paradigm

Alexis P. Malozemoff

IBM Thomas J. Watson Research Center, P.O. Box 218, Yorktown Heights, New York 10598

(Received 21 February 1986)

Earlier atomic d -state models of anisotropic magnetoresistance $\Delta\rho/\rho$ are reviewed and found to suffer from a weak-ferromagnetism "catastrophe": a nonphysical finite value of $\Delta\rho/\rho$ as exchange splitting goes to zero. New calculations of $\Delta\rho/\rho$, including cubic anisotropy, avoid this problem and offer a new paradigm for interpreting experiments on systems with various band structures: dilute polycrystalline nickel alloys with virtual-bound-state (VBS) and non-VBS impurities, and also weak concentrated ferromagnets like Fe-Ni Invar. p states are also found to give nonzero $\Delta\rho/\rho$ in an atomic model.

I. INTRODUCTION

The anisotropic magnetoresistance measures the difference in resistivity ρ when the magnetization vector of a single-domain ferromagnet in zero field lies either parallel (\parallel) or perpendicular (\perp) to the current:

$$\Delta\rho/\rho = (\rho_{\parallel} - \rho_{\perp})/\rho_{av}, \quad (1)$$

where ρ_{av} is an appropriate average of the parallel and perpendicular resistivities.¹ The most successful microscopic theories of this effect,²⁻⁴ applied to a variety of moderately dilute alloys, rest on an astonishingly simple atomic d -state model which incorporates spin-orbit coupling and exchange splitting but which appears to ignore a more realistic band structure. On the other hand, efforts to take into account the band structure⁵⁻⁷ have by and large led to complex results which do not illuminate the apparent simplicity of the experimental data.^{4,8,9}

In this paper, I introduce several basic concepts which help bridge the gap between the atomic models and a more realistic band structure. In particular, in addition to spin-orbit coupling and exchange splitting, the ligand field effect is an essential ingredient in the physics of anisotropic magnetoresistance. While ligands in principle give rise to all the complexity of band structure, I model their effect in the simplest possible way, namely as a cubic anisotropy. I show how a new calculation including cubic anisotropy offers a simple paradigm for improving our understanding of a mass of experimental data. I also consider the phenomenon of weak ferromagnetism, in which exchange splitting becomes small; this reveals a serious flaw in some earlier work and clarifies the role of the exchange splitting in the overall theory.

The paper is structured as follows. First, in Sec. II, I review the experimental data of interest and introduce the phenomenological framework for the discussion: Mott's two-current sd -scattering model¹⁰ and Muth and Christoph's formulas¹¹ for $\Delta\rho$. Crucial here is the notion that the band structure of each individual case determines the parameters of these formulas. I show how Muth and Christoph, among others, did not adequately take this into

account. In particular I contrast the band structures of systems with and without impurity virtual bound states (VBS's) and also strong versus weak ferromagnets.

Next, in Sec. III, I reconsider the Smit spin mixing² and $L_z S_z$ atomic models of $\Delta\rho$, as developed by Campbell *et al.*³ and Jaoul *et al.*,⁴ which have so far served, in general, as the paradigms for understanding experiment. Among other problems, these theories give unphysical finite results in the limit of zero exchange splitting. This may be termed a "weak-ferromagnetism catastrophe."

In Sec. IV, I present new calculations of $\Delta\rho/\rho$ in the atomic model: for d states in the presence of cubic anisotropy, and also for p states. The cubic-anisotropy calculations introduce, in the simplest possible way, a ligand field effect into the atomic model. As Berger⁵ and Potter⁷ first recognized, some kind of ligand effect, whether cubic anisotropy or band splittings in some other form, is an essential feature of any physically plausible model for anisotropic magnetoresistance. Indeed, I show that the cubic-anisotropy results avoid the weak-ferromagnetism catastrophe and so offer an improved paradigm for understanding experiment.

Finally, in Sec. V, I review the band model of anisotropic magnetoresistance and introduce the concept of "band averaging" over atomic d states. Then I treat three cases of experimental interest: non-VBS impurities in nickel, weakly ferromagnetic Fe-Ni Invar, and VBS impurities in nickel. In each case the cubic anisotropy paradigm offers a novel, and in some ways more satisfactory, interpretation of the data, although agreement is still semiquantitative at best. Some preliminary discussion of the weakly ferromagnetic case was given earlier.¹²

II. REVIEW OF PHENOMENOLOGICAL THEORY AND EXPERIMENTAL RESULTS

The framework for understanding the galvanomagnetic properties of nickel alloys is Mott's well-known two current sd -scattering model.¹⁰ At low temperatures, conduction occurs by s and d electrons which can be divided into up-spin (majority) or down-spin (minority) channels. While the resistivities ρ^{\uparrow} and ρ^{\downarrow} of the two channels act in

parallel, within each channel resistivity ρ_s from scattering off s - and p -potential perturbations is usually considered to add in series to resistivity ρ_d due to scattering from d -state perturbations. If significant d -state density is present at the Fermi surface, ρ_d is usually much stronger than ρ_s in crystalline transition-metal alloys. In principle, resistance anisotropy $\Delta\rho$ can occur in either channel. To lowest order in this anisotropy, one can then write⁸

$$\frac{\Delta\rho}{\rho} = \frac{\rho^\uparrow}{\rho^\uparrow + \rho^\downarrow} \left[\frac{\Delta\rho^\uparrow}{\rho^\uparrow} \right] + \frac{\rho^\downarrow}{\rho^\uparrow + \rho^\downarrow} \left[\frac{\Delta\rho^\downarrow}{\rho^\downarrow} \right]. \quad (2)$$

Experimental anisotropic magnetoresistance ratios^{4,8} are approximately independent of concentration for moderately dilute polycrystalline nickel alloys (2–20% impurity); results are summarized in Table I. Data on more concentrated nickel-iron alloys⁹ are shown in Fig. 1. Schematic d -band densities of states are shown for NiFe and NiCr alloys in Fig. 2.

Let us first consider the strongly ferromagnetic alloys of Ni with moderately dilute Mn, Fe, Co, Zn, Cu, and Au. In these cases, to a first approximation, there is no d density at the up-spin Fermi surface, as shown in Fig. 2(a). Thus, ρ^\uparrow is just ρ_s , which is of order $1 \mu\Omega \text{ cm/at. \%}$ or less for the transition-metal impurities in Table I. On the other hand, ρ^\downarrow , which is dominated by ρ_d , ranges from 2.6 to $5.2 \mu\Omega \text{ cm/at. \%}$. The remarkable constancy of these values (to within a factor of 2) can be traced to the fact that the impurity d states lie predominantly above [e.g., Fe; see Fig. 1(a)] or below (e.g., Cu) the nickel states.

TABLE I. Experimental majority ($up\uparrow$) spin and minority (down \downarrow) spin resistivities ρ and anisotropic magnetoresistance ratios $\Delta\rho/\rho$ for dilute impurities in nickel at $T \sim 0 \text{ K}$, from Dorleijn.⁸ VBS means virtual bound state.

Impurity	ρ^\uparrow ($\mu\Omega \text{ cm/at \%}$)	ρ^\downarrow ($\mu\Omega \text{ cm/at \%}$)	$\Delta\rho^\uparrow/\rho^\uparrow$ (%)	$\Delta\rho^\downarrow/\rho^\downarrow$ (%)	$\Delta\rho/\rho$ (%)
Impurities with no VBS					
²⁵ Mn	0.83	5.2	1.5	10	-3.2
²⁶ Fe	0.44	4.8	1.2	14	-2.2
²⁷ Co	0.20	2.6	1.1	15	-1.5
²⁹ Cu	1.3	3.8	3.3	10	-2.0
³⁰ Zn	1.3	2.9	3.3	8	-2.8
⁷⁹ Au	0.44	2.6	1.3	9	-2.1
²³ Al	3.4	5.8	4.2	7	-2.2
¹⁴ Si	5.0	6.4	4.7	6	-3.1
⁵⁰ Sn	4.4	7.2	3.8	6	-2.6
Impurities with VBS					
²² Ti	7.6	7.2	4.3	4.1	-3.1
²³ V	14	6.4	17	7.8	-3.0
²⁴ Cr	29	6.1	27	5.7	-1.7
⁴⁴ Ru	72	5.4	99	7.4	-1.1
⁴⁵ Rh	8	2.3	26	7.5	-2.3
⁷⁵ Re	24	7.5	20	6.2	-2.3
⁷⁷ Ir	21	5.0	-10	-2.4	-1.4
⁷⁸ Pt	3.6	0.85	24	5.7	-0.8

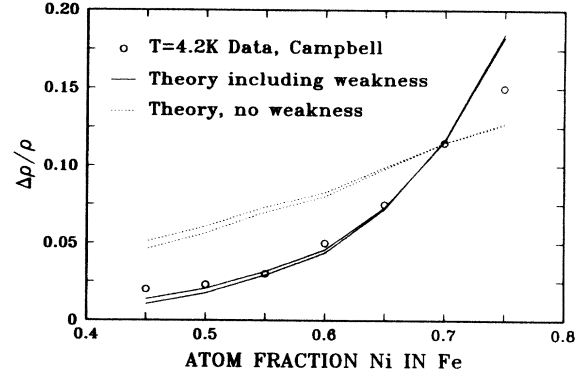


FIG. 1. Anisotropic magnetoresistance ratio $\Delta\rho/\rho$ of Ni-Fe polycrystalline alloys. Circles are data of Campbell (Ref. 9). Solid lines are predictions from Eq. (9) including weak ferromagnetism and bandwidth changes as a function of composition, as discussed in Sec. VC. Dotted lines are predictions ignoring these effects (Ref. 12). Upper and lower curves of each pair correspond to $\gamma = 0.005$ and 0.01 , respectively, at $x_{\text{Ni}} = 0.7$.

Therefore, at the Fermi energy, where scattering occurs, these impurities look simply like a hole in the nickel band, which is roughly the same, whatever the impurity. The $\Delta\rho^\uparrow$ and $\Delta\rho^\downarrow$ values which can be determined independently⁸ by studies of deviations from Matthiessen's rule,¹³ also show a remarkable overall consistency. Normalized by ρ^\downarrow , they are all $+2 \pm 1\%$ and $-2 \pm 1\%$, respectively. This suggests that both $\Delta\rho^\uparrow$ and $\Delta\rho^\downarrow$ are somehow related to ρ^\downarrow but not to ρ^\uparrow .

The nickel alloys with Al, Si, and Sn are still strongly ferromagnetic but have noticeably larger ρ^\uparrow (see Table I),

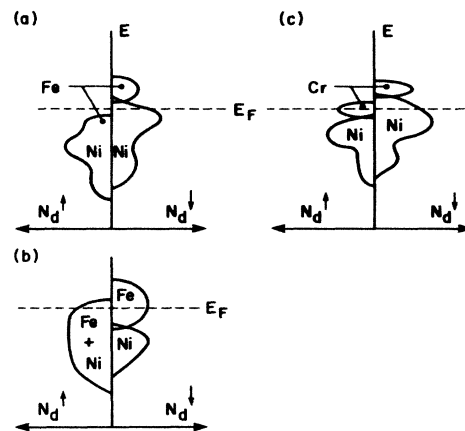


FIG. 2. Schematic up-spin (majority) and down-spin (minority) d -band densities of states N_d versus energy for (a) moderately dilute Fe in Ni, (b) concentrated Fe-Ni Invar and (c) moderately dilute Cr in Ni. The relatively sharp up-spin Cr peak at E_F is known as a "virtual bound state" (VBS), while the two Ni-Fe cases illustrate (a) "strong" and (b) "weak" ferromagnetism, respectively.

which presumably arises from stronger sp scattering. Correspondingly, $\Delta\rho^\uparrow/\rho^\uparrow$ is noticeably larger than in the first group of alloys.

It is known that for Fe-Ni alloys with Fe concentration above about 20% (permalloy), the Fermi level enters the down-spin iron band.¹⁴ Above about 50%, the exchange splitting is insufficient to keep the d bands fully polarized.¹⁵ In other words d -state density appears at the up-spin Fermi surface as in Fig. 2(b). This condition is known as weak ferromagnetism. While $\Delta\rho^\uparrow$ and $\Delta\rho^\downarrow$ have not been independently determined in this region, $\Delta\rho/\rho$ falls to low values with increasing iron as shown in Fig. 1, while both specific heat and resistivity increase rapidly.¹⁵

The "virtual-bound-state" (VBS) alloys of Ni with Ti, V, Cr, Ru, Rh, Re, Ir, and Pt have d density at the up-spin Fermi surface,¹⁶ as shown in Fig. 2(c). Because this peak is relatively sharp, the density of states is high, which causes large scattering in the up-spin channel and explains the huge ρ^\uparrow values in Table I. ρ^\uparrow remains in the same range as before, being dominated by nickel d -hole scattering, and so $\Delta\rho^\uparrow/\rho^\uparrow$ has values $-2\pm 1\%$ similar to the first group. But $\Delta\rho^\downarrow/\rho^\downarrow$ shows a tremendous range of values. $\Delta\rho^\downarrow/\rho^\downarrow$ is somewhat better behaved, being typically $6\pm 2\%$ except for In with -2.9 , for this data of Dorleijn⁸ (Jaoul *et al.*⁴ have somewhat more variability in their values). In summary, in contrast to the non-VBS alloys, these alloys appear to have $\Delta\rho^\uparrow$ related to ρ^\uparrow , not to ρ^\downarrow .

To explore the origin of these trends in $\Delta\rho^\uparrow$ and $\Delta\rho^\downarrow$, we use the relations proposed by Muth and Christoph:¹¹

$$\Delta\rho^\uparrow = \gamma_2\rho_d^\downarrow - \gamma_1\rho_d^\uparrow, \quad (3)$$

$$\Delta\rho^\downarrow = \gamma_1'\rho_d^\uparrow - \gamma_2'\rho_d^\downarrow, \quad (4)$$

where the four γ 's are constants. The underlying assumption of these relations is simply that any resistance anisotropy is related to scattering off d states and hence to ρ_d^\uparrow and ρ_d^\downarrow . Then the right-hand side of Eqs. (3) and (4) can be interpreted as merely the first, or linear, terms in an expansion in ρ_d .

Muth and Christoph combined Eqs. (2)–(4) and attempted to fit $\Delta\rho/\rho$ data on all the nickel alloys of Table I with a single set of γ parameters. Taking $\gamma_1'/\gamma_1 = \gamma_2'/\gamma_2$, they obtained $\gamma_1 = -4.25\%$, $-\gamma_1' = 0.21\%$, $\gamma_2 = 1\%$, and $\gamma_2' = 0.048\%$. They did not, however, consider the more detailed experimental data on $\Delta\rho^\uparrow$ and $\Delta\rho^\downarrow$ separately, and comparison with Table I shows their results cannot possibly be correct. For example, for the strongly ferromagnetic alloys where $\rho_d^\downarrow = 0$ we can identify $\Delta\rho^\uparrow/\rho^\uparrow \sim \gamma_2 \sim 2\%$ and $\Delta\rho^\downarrow/\rho^\downarrow \sim -\gamma_2' \sim -2\%$ in Table I; so $\gamma_2/\gamma_2' \sim 1$ while Muth and Christoph found $\gamma_2/\gamma_2' \sim 21$. For the virtual-bound-state alloys, since $\Delta\rho^\uparrow/\rho^\uparrow$ remains about the same, it is reasonable to presume from Eq. (4) that $\gamma_2' \sim 2\%$ is the same as in the strongly ferromagnetic alloys while $\gamma_1' \sim 0$. But the large values of $\Delta\rho^\downarrow/\rho^\downarrow$ suggest that $\gamma_1 \sim$ varies from -3 to $+8\%$. Since $\rho_d^\downarrow/\rho_d^\uparrow$ is small in many virtual-bound-state alloys, Eq. (3) does not allow determination of γ_2 which most likely remains at 2% (see Sec. V D).

The reason for the above discrepancies between the data and the fit of Muth and Christoph will become clear in

Secs. III–V, where microscopic derivations show that the γ 's depend on details of the band structure. Thus, it is inappropriate to lump all the data together as Muth and Christoph attempted to do. Nevertheless, we shall see that for certain groups of alloys with similar band structure, their formula is indeed useful and the systematics in the values of γ can be understood at least approximately from first principles.

III. ATOMIC THEORY OF ANISOTROPIC MAGNETORESISTANCE AND THE WEAK-FERROMAGNETISM CATASTROPHE

A. Smit spin-mixing mechanism

The microscopic theory of anisotropic magnetoresistance properly began with the work of Smit,² who pointed out that the effect depended on spin-orbit coupling, the Hamiltonian of which can be written

$$A \mathbf{L} \cdot \mathbf{S} = A L_z S_z + \frac{1}{2} A (L_+ S_- + L_- S_+), \quad (5)$$

where A is the spin-orbit coupling constant, \mathbf{L} and \mathbf{S} are the orbital and spin angular momentum operators, and L_+ and L_- , etc., are the usual raising and lowering operators.

Smit considered an atomic d -state manifold of ten states $|i\rangle$, whose identifications and angular components are listed for future reference in Table II, along with the spin-orbit matrix elements. These states are split into two fivefold degenerate groups by an exchange field H , with Hamiltonian $-\mathbf{H} \cdot \mathbf{S}$, where H includes the gyromagnetic ratio and Bohr magneton. In the matrix of Table II, this term would introduce $H/2$ on the diagonal for the first five states and $-H/2$ on the diagonal for the last five states. Ignoring the $L_z S_z$ term of Eq. (5) (to which we will return below), and focusing on the remaining terms, Smit noted that in the matrix of Table II, those terms gave off-diagonal matrix elements which mixed the fivefold spin-up with the fivefold spin-down manifold. To first order in perturbation theory (i.e., to order $\epsilon = A/H$) he calculated the admixture of up-spin states into the down-spin manifold, finding that the admixtures were weighted unevenly among the five states.

Next Smit assumed that the Fermi level lay at the down-spin d manifold and considered that up- or down-spin conduction electrons $|k\rangle$ scattered off the d states, giving rise to a resistivity which he crudely estimated by the square of a scattering matrix element $\langle k | V | i \rangle$. This approximation will also be used in this paper. Because of the asymmetric admixtures of up-spin states, Smit found different scattering in the up-spin channel for \mathbf{k} parallel or perpendicular to \mathbf{H} . Squaring the matrix element causes the difference $\Delta\rho$ to depend in second order [$\epsilon^2 = (A/H)^2$] on the spin-orbit coupling. This is known as the Smit or spin-mixing mechanism of anisotropic magnetoresistance.

Subsequently, Campbell, Fert, and Jaoul³ improved Smit's calculation by noticing that since this was a second-order effect, it was necessary to go to second order in the wave functions before calculating the resistivity. In effect a second-order normalization condition on the

TABLE II. Angular parts of d wave functions $|i\rangle$ with spin down (\downarrow is the minority) and spin up (\uparrow is the majority), and the spin-orbit coupling matrix $\mathbf{AL}\cdot\mathbf{S}$ normalized by $A/2$.

	1	2	3	4	5	6	7	8	9	10
1= $yz\downarrow$	0	$-i$	0	0	0	0	0	1	$-i$	$-i\sqrt{3}$
2= $zx\downarrow$	i	0	0	0	0	0	0	i	1	$-\sqrt{3}$
3= $xy\downarrow$	0	0	0	$-2i$	0	-1	$-i$	0	0	0
4= $[(x^2-y^2)/2]\downarrow$	0	0	$2i$	0	0	i	-1	0	0	0
5= $[(3z^2-r^2)/2\sqrt{3}]\downarrow$	0	0	0	0	0	$i\sqrt{3}$	$\sqrt{3}$	0	0	0
6= $yz\uparrow$	0	0	-1	$-i$	$-i\sqrt{3}$	0	i	0	0	0
7= $zx\uparrow$	0	0	$+i$	-1	$\sqrt{3}$	$-i$	0	0	0	0
8= $xy\uparrow$	1	$-i$	0	0	0	0	0	0	$2i$	0
9= $[(x^2-y^2)/2]\uparrow$	i	1	0	0	0	0	0	$-2i$	0	0
10= $[(3z^2-r^2)/2\sqrt{3}]\uparrow$	$i\sqrt{3}$	$-\sqrt{3}$	0	0	0	0	0	0	0	0

zeroth-order wave function¹⁷ introduced a resistivity anisotropy of similar magnitude but opposite sign in the minority-spin channel. This normalization has unfortunately been overlooked in theoretical work by other authors but will be included in what follows.

For future reference, Table III shows the resistivities of the five primarily spin-down eigenstates to second order, as calculated in the Campbell *et al.* model,³ but including also the zeroth-order effects coming from the $L_z S_z$ term of Eq. (5). These resistivities are normalized to the zeroth-order (no spin-orbit) down-spin resistivity ρ_{d0} . Very similar results apply for the five primarily spin-up eigenstates if it is assumed the Fermi level lies opposite them. All the terms of order ϵ^2 in the table come from the Smit spin-mixing mechanism. Summed over the five states (i.e., ignoring the first-order splittings), $\Delta\rho/\rho_{d0}$ can be seen to give $\pm 3\epsilon^2/4$ for the two channels, independent of impurity concentration. For the other five primarily spin-up states, the net $\Delta\rho^\downarrow$ and $\Delta\rho^\uparrow$ turn out to have the same magnitude but opposite signs.

In the case of a strong ferromagnet, ρ_d^\downarrow is zero and ρ_{d0} corresponds to ρ_d^\downarrow ; so one can identify $\gamma_2 = \gamma_2' = +3\epsilon^2/4$ in the Muth-Christoph formulas Eqs. (3) and (4). Substituting in Eq. (2) and assuming an isotropic scattering ρ_s in both spin-up and spin-down channels, one finds

$$\begin{aligned} \Delta\rho/\rho &= \gamma\rho_d^{\downarrow 2}/\rho^\downarrow\rho^\uparrow \\ &= \gamma\alpha \left[1 - \frac{1}{\alpha}\right]^2, \end{aligned} \quad (6)$$

with

$$\begin{aligned} \gamma &= 3\epsilon^2/4 = 3A^2/4H^2, \\ \rho^\downarrow &= \rho_s, \\ \rho^\uparrow &= \rho_d^\uparrow + \rho_s, \\ \alpha &= \rho^\downarrow/\rho^\uparrow. \end{aligned}$$

This differs from the well-known result of Campbell *et al.*³

$$\Delta\rho/\rho = \gamma(\alpha - 1), \quad (7)$$

which can be derived if isotropic scattering is completely neglected in the spin-down channel, i.e., $\rho^\downarrow = \rho_d^\downarrow$. Since ρ^\downarrow and ρ^\uparrow are both proportional to impurity concentration in the moderately dilute regime, both Eqs. (6) and (7) predict $\Delta\rho/\rho$ to be independent of concentration.

Thus Campbell *et al.*³ beautifully explained (1) the concentration independence, (2) the opposite signs of $\Delta\rho^\downarrow/\rho^\downarrow$ and $\Delta\rho^\uparrow/\rho^\uparrow$, and (3) their approximate constancy, for the

TABLE III. Second-order eigenenergies E and resistivities ρ for the five primarily spin-down d eigenstates of a Hamiltonian with exchange field \mathbf{H} and spin-orbit coupling A ($\epsilon = A/H$). $\Delta\rho = \rho_{\parallel} - \rho_{\perp}$, and ρ_{d0} is resistivity without spin-orbit coupling.

State	1	2	3	4	5	Sum
$E/H - \frac{1}{2}$	$-\epsilon + \epsilon^2$	$-\epsilon/2 + 3\epsilon^2/2$	$3\epsilon^2/2$	$\epsilon/2 + \epsilon^2$	ϵ	
$\rho_{\parallel}^\downarrow/\rho_{d0}$		$3\epsilon^2/2$				
$\rho_{\perp}^\downarrow/\rho_{d0}$		$3\epsilon^2/8$		$3\epsilon^2/8$		
$\Delta\rho^\downarrow/\rho_{d0}$		$9\epsilon^2/8$		$-3\epsilon^2/8$		$3\epsilon^2/4$
$\rho_{\parallel}^\uparrow/\rho_{d0}$			$1 - 3\epsilon^2/2$			
$\rho_{\perp}^\uparrow/\rho_{d0}$	$\frac{3}{8} - 3\epsilon^2/8$		$\frac{1}{4} - 3\epsilon^2/8$		$\frac{3}{8}$	
$\Delta\rho^\uparrow/\rho_{d0}$	$-\frac{3}{8} + 3\epsilon^2/8$		$\frac{3}{4} - 9\epsilon^2/8$		$-\frac{3}{8}$	$-3\epsilon^2/4$

set of strongly ferromagnetic non-VBS nickel alloys in Table I. Even the magnitude of γ , estimated to be of order 0.01, was about right. In an equivalent test of the theory, they plotted the net $\Delta\rho/\rho$ versus α according to Eq. (7) and found an approximately linear dependence for the different systems, as long as $\alpha \geq 1$ (the non-VBS alloys). It should be noted that in the limit of large α , Eqs. (6) and (7) reduce to $\gamma(\alpha-2)$ and $\gamma(\alpha-1)$, respectively, and so do not differ substantially within experimental scatter. For small α on the other hand, Eq. (6) is always positive while Eq. (7) becomes negative. However, neither of these equations accounts adequately for the data on systems with $\alpha < 1$ (the VBS alloys) and other mechanisms will be discussed below for these cases.

While the theory of Campbell *et al.* gives the most quantitative and comprehensive explanation of anisotropic magnetoresistance data to date, several questions remain: The basic one is how can such a simple atomic d -state model apply in the context of a realistic band structure? A more specific and perhaps even more serious question is: How can $\Delta\rho/\rho$ go as $\gamma=3A^2/4H^2$, which diverges as exchange field $H \rightarrow 0$?

An $H \rightarrow 0$ "catastrophe" remains even if one attempts to generalize the spin-mixing model to the weak-ferromagnetic limit where both up-spin and down-spin d -state densities appear at the Fermi surface.

In the low exchange-field limit, the difference in up- and down-spin d -state densities, and hence the difference in up- and down-spin d resistivities, goes linearly with H . To lowest order¹²

$$\Delta\rho^{\uparrow,\downarrow} = \pm\gamma(\rho_d^{\downarrow} - \rho_d^{\uparrow}), \quad (8)$$

where the signs come directly from Table III and the corresponding spin-up calculation. In the notation of Muth and Christoph, this corresponds to $\gamma_2 = \gamma'_2 = \gamma_1 = \gamma'_1 = \gamma$. Substituting in Eq. (2), one finds¹²

$$\Delta\rho/\rho = \gamma(\rho_d^{\downarrow} - \rho_d^{\uparrow})/\rho^{\uparrow}. \quad (9)$$

Since $\rho_d^{\downarrow} - \rho_d^{\uparrow} \propto H$ but $\gamma \propto 1/H^2$, $\Delta\rho/\rho$ approaches a constant as $H \rightarrow 0$, at least down to a field energy comparable to the spin-orbit energy. But physically one would expect $\Delta\rho/\rho$ to approach zero as magnetism disappears. We will return to this problem below.

B. $L_z S_z$ MECHANISM

Berger⁵ first emphasized that in addition to the Smit mechanism, the $L_z S_z$ terms of the spin-orbit coupling can in themselves give rise to anisotropic magnetoresistance. Berger considered the case of a hypothetical near-degeneracy in the band structure, but Jaoul *et al.*⁴ pointed out that the effect can most clearly be seen in the simple atomic d -state model introduced above: The $L_z S_z$ terms in the matrix of Table II generate zeroth-order contributions to $\Delta\rho^{\uparrow}$ for three of the primarily spin-down states; these are the $-\frac{3}{8}$, $\frac{3}{4}$, and $-\frac{3}{8}$ terms in Table III. Identical values are obtained for $\Delta\rho^{\uparrow}$ in the primarily spin-up manifold. If the first-order energy splittings are ignored and the states taken as effectively degenerate, the net effect, reflected in the sum over these values, is zero.

However, Jaoul *et al.*⁴ showed that, if the splittings are

not ignored, broadening of the component levels to a width W larger than the spin-orbit splitting A leads to $\Delta\rho$ with amplitude of order $(A/W)^2$, exhibiting a negative-positive-negative pattern as a function of the Fermi level position in the band. This mechanism, which can be dubbed the $L_z S_z$ mechanism, differs from Smit's spin-mixing mechanism because it arises from a *single* spin channel, up or down. Thus, the spin-mixing mechanism is, as the name implies, as *interchannel* effect, while the $L_z S_z$ mechanism is an *intrachannel* effect.

The simple systematics of experimental data on non-VBS alloys in Table I, especially the roughly equal magnitudes and opposite signs of $\Delta\rho^{\downarrow}/\rho^{\downarrow}$ and $\Delta\rho^{\uparrow}/\rho^{\uparrow}$, pointed strongly towards the spin-mixing mechanism, as discussed above. In view of this, Berger's original application⁵ of the $L_z S_z$ mechanism to permalloy (NiFe alloys) seems, in retrospect, inappropriate. By contrast, the $\Delta\rho^{\downarrow}/\rho^{\downarrow}$ values for VBS impurities in Table I have no negative counterpart in $\Delta\rho^{\uparrow}/\rho^{\uparrow}$ and thus these systems are more likely candidates for the $L_z S_z$ mechanism, as first pointed out by Jaoul *et al.*⁴ They suggested that the virtual bound states in the up-spin band [see Fig. 2(c)] are responsible.

More specifically, Jaoul *et al.*⁴ included both the Smit effect coming from the down-spin nickel band and the $L_z S_z$ effect coming from the spin-up VBS:

$$\Delta\rho^{\downarrow} = \gamma\rho_d^{\downarrow} + 3\beta\rho_d^{\downarrow}, \quad \Delta\rho^{\uparrow} = -\gamma\rho_d^{\uparrow}, \quad (10)$$

where 3β , of order $(A/W)^2$, represents the $L_z S_z$ effect. Once again the Muth-Christoph parameters find different values: $\gamma_2 = \gamma'_2 = \gamma$, $\gamma_1 = 3\beta$, $\gamma'_1 = 0$. Substituting Eqs. (10) in Eq. (2) and ignoring ρ_s in both channels, Jaoul *et al.* obtained

$$\Delta\rho/\rho = \gamma(\alpha - 1) + 3[\alpha/(\alpha + 1)]\beta. \quad (11)$$

Comparing to experiment they found effects of the correct order of magnitude, but with imperfect agreement in detail. Only the $5d$, but not the $3d$ or $4d$, series showed some negative values which are expected as part of a negative-positive-negative pattern.

There are also more fundamental questions. As before, one must wonder how band structure can be ignored. There is also an $H \rightarrow 0$ catastrophe: Although $\beta \propto (A/W)^2$ does not diverge as $H \rightarrow 0$ [as $\gamma \propto (A/H)^2$ does in the spin mixing case], both $\Delta\rho^{\downarrow}/\rho^{\downarrow}$ and $\Delta\rho^{\uparrow}/\rho^{\uparrow}$ approach the same value according to the results in Table III and the corresponding spin-up calculation. Then Eq. (2) predicts a constant $\Delta\rho/\rho$ as $H \rightarrow 0$, which is physically implausible as before.

Yet another problem is that according to Table III, the virtual bound states should give a spin-mixing effect. Thus

$$\begin{aligned} \Delta\rho^{\downarrow} &= \gamma_N \rho_d^{\downarrow} - \gamma_v \rho_d^{\downarrow} + 3\beta \rho_d^{\downarrow}, \\ \Delta\rho^{\uparrow} &= -\gamma_N \rho_d^{\uparrow} + \gamma_v \rho_d^{\uparrow}, \end{aligned} \quad (12)$$

where γ_N and γ_v represent values for the nickel host and the virtual bound states, respectively. Then Eq. (2) leads to

$$\frac{\Delta\rho}{\rho} = \gamma_N(\alpha - 1) + \gamma_v \left[\frac{1}{\alpha} - 1 \right] + 3\beta \frac{\alpha}{1 + \alpha}. \quad (13)$$

For Cr and other 3d VBS transition metals, γ_v is expected to be comparable to γ_N ; for the 4d and 5d series it will be even larger. Furthermore, for all the VBS impurities in Table I, $\alpha = \rho^1/\rho^1$ is substantially less than 1. Then the γ_v/α term in Eq. (13) can be expected to dominate, drastically changing the original predictions of Jaoul *et al.*⁴ In the case of Cr for example, taking $\gamma_v = 2\%$, one finds $\gamma_v/\alpha \sim 2 \times 29/6.1 = 9.7\%$, which is positive and large, clearly disagreeing with Eq. (11) and the data for $\Delta\rho^1/\rho^1$ in Table I, which are negative and small.

IV. NEW PREDICTIONS OF THE ATOMIC THEORY: CUBIC ANISOTROPY AND p STATES

A. Cubic anisotropy

A cubic anisotropy will modify the atomic d -state calculation of anisotropic magnetoresistance. Marsocci¹⁸ first attempted such a calculation, but incorrectly, as subsequently admitted by Thomas, Marsocci, and Lin.¹⁹ The latter authors, however, did not correct the calculation, choosing rather to focus on fourth-order terms in the spin-orbit coupling, which are unnecessary in the present context. Berger and Friedburg⁶ also introduced cubic anisotropy, but in a phenomenological rather than microscopic way. Here I present a calculation for cubic anisotropy using the atomic model. In many respects it is similar to the work of Potter,⁷ although it corrects spin-orbit matrix elements (compare Table II with the corresponding Table II of Ref. 7), includes the all-important normalization terms, and is not specific to the particular d -state structure which Potter assumed at the top of the nickel band. For whichever of these reasons, Potter's results concerning the relative magnitudes and signs of spin-up and spin-down contributions were in complete contradiction to the experimental results of Table I, while as shall be seen, the results obtained in the present paper agree quite well.

To carry out this calculation for current along the [100] cubic axes, the cubic splitting K is introduced on the diagonal in the matrix of Table II. Specifically the $x^2 - y^2$

and $3z^2 - r^2$ d -state energies are shifted up by K , leaving the other states unchanged. Next the yz and zx states are re-diagonalized, as first suggested by Potter,⁷ to eliminate the need for degenerate perturbation theory. Finally perturbation theory is carried out to second order and the resistivities for currents along [100] and [010] or [001] are calculated, giving the results in Tables IV and V for the primarily spin-up and spin-down eigenstates, respectively. Here $|H - K|$, $|K|$, and $|H|$ must be assumed larger than A . In particular the results hold for H larger than K and for K larger than H , both of which cases will be important in the discussion which follows. A sum over the doublets and triplets of the cubic symmetry is given in Table VI. This key table will be the basis for comparison to experiment in subsequent sections.

Several features of these results are noteworthy. As $K \rightarrow 0$, Table VI reduces to the $\pm 3\epsilon^2/4$ of the simple Smit spin-mixing mechanism. However for finite K these terms evolve into the $3\epsilon_{\pm}^2/4 = 3A^2/4(H \pm K)^2$ terms of Table VI, which recall the kinds of denominators Potter⁷ obtained in his calculation. The origin of these terms can be traced back to both interchannel and intrachannel ($L_z S_z$) spin-orbit matrix elements; in other words they are not pure Smit spin-mixing terms. On the other hand they have a form similar to the original Smit spin-mixing calculation of Campbell *et al.*,³ and so they may be termed "pseudo-spin-mixing" terms. Interestingly, the simple pattern of opposite signs and equal magnitudes of $\Delta\rho^1$ is broken. What is more, for any given spin group of Table VI, the pseudo-spin-mixing terms are confined to either $\Delta\rho^1$ or $\Delta\rho^1$ but not both. This feature, however, is specific to the [100] and [010] directions assumed for the electric current.

In addition to the pseudo-spin-mixing terms, new terms in $\delta (= A/K)$ appear in Table VI, which can be traced exclusively to the $L_z S_z$ effect. Now the characteristic negative-positive-negative pattern and the amplitude of order $(A/W)^2$, predicted by Jaoul *et al.*,⁴ are replaced by negative and positive $3\delta^2/4$ terms for the triplet and doublet, respectively. This result is a concrete example of the earlier rather general argument of Berger⁵ that a band

TABLE IV. Second-order eigenenergies E and resistivities ρ (current || [100]) for the five primarily spin-down d eigenstates of a Hamiltonian with exchange field H , spin-orbit coupling A ($\epsilon = A/H$), and cubic anisotropy K [$\delta = A/K$, $\epsilon_+ = A/(H + K)$, $\epsilon_- = A/(H - K)$]. Other notation as in earlier tables, except that states 1 and 2 represent, to first order, the orbital states $m_z = \mp 1$, respectively.

State	1	2	3	4	5
$E/H - \frac{1}{2}$	$(\epsilon + \epsilon^2 + \epsilon\epsilon_-)/2$	$(-\epsilon + 3\epsilon\epsilon_-)/2$	$-\epsilon\delta + \epsilon^2/2$	$\epsilon/\delta + \epsilon\delta + \epsilon\epsilon_+/2$	$\epsilon/\delta + 3\epsilon\epsilon_+/2$
$\rho_{ }^1/\rho_{d0}$		$3\epsilon_-^2/2$			
ρ_{\perp}^1/ρ_{d0}	$3\epsilon_-^2/8$	$3\epsilon_-^2/8$			
$\Delta\rho^1/\rho_{d0}$	$-3\epsilon_-^2/8$	$9\epsilon_-^2/8$			
$\rho_{ }^1/\rho_{d0}$					$1 - 3\epsilon_+^2/2$
ρ_{\perp}^1/ρ_{d0}			$3\delta^2/4$	$3(1 - \delta^2 - \epsilon_+^2)/4$	$\frac{1}{4} - 3\epsilon_+^2/8$
$\Delta\rho^1/\rho_{d0}$			$-3\delta^2/4$	$-3(1 - \delta^2 - \epsilon_+^2)/4$	$\frac{3}{4} - 9\epsilon_+^2/8$

TABLE V. As in Table IV, second-order eigenenergies E and resistivities ρ (current \parallel [100]) for the five primarily spin-up d eigenstates of the Hamiltonian with cubic anisotropy. States 6 and 7 represent, to first order, the orbital states. $m_z = \mp 1$.

State	6	7	8	9	10
$E/H + \frac{1}{2}$	$-(\epsilon - 3\epsilon\epsilon_+)/2$	$(\epsilon - \epsilon^2 - \epsilon\epsilon_+)/2$	$-\epsilon\delta - \epsilon^2/2$	$\epsilon/\delta + \epsilon\delta - \epsilon\epsilon_-/2$	$\epsilon/\delta - 3\epsilon\epsilon_-/2$
$\rho_{ }^\dagger/\rho_{d0}$					$1 - 3\epsilon_-^2/2$
$\rho_{\perp}^\dagger/\rho_{d0}$			$3\delta^2/4$	$3(1 - \delta^2 - \epsilon_-^2)/4$	$\frac{1}{4} - 3\epsilon_-^2/8$
$\Delta\rho^\dagger/\rho_{d0}$			$-3\delta^2/4$	$-3(1 - \delta^2 - \epsilon_-^2)/4$	$\frac{3}{4} - 9\epsilon_-^2/8$
$\rho_{ }^\dagger/\rho_{d0}$	$3\epsilon_+^2/2$				
$\rho_{\perp}^\dagger/\rho_{d0}$	$3\epsilon_+^2/8$	$3\epsilon_+^2/8$			
$\Delta\rho^\dagger/\rho_{d0}$	$9\epsilon_+^2/8$	$-3\epsilon_+^2/8$			

splitting D can lead to contributions to $\Delta\rho$ of order $(A/D)^2$.

Another interesting concept which arises from these results is that of the *quenching* of $L_z S_z$ contributions to $\Delta\rho$ by the cubic anisotropy, a concept somewhat analogous to the well-known orbital angular momentum quenching effect. Without the cubic anisotropy, Table III shows zeroth-order contributions to $\Delta\rho$ spaced by first-order energy shifts. The corresponding cubic calculation in Tables IV and V shows these terms quenched to give only a second-order contribution $(A/K)^2$. The remaining zeroth-order terms ($\pm \frac{3}{4}$) now appear in the doublets (states 4 and 5 or 9 and 10) of Tables IV and V, and because their energies differ only to second order in A , these terms can effectively be summed to zero.

An important feature of the results in Table VI is that now the weak-ferromagnetic catastrophe is eliminated. For example, considering the triplet states to lie close to the Fermi level as $H \rightarrow 0$, Table VI implies

$$\Delta\rho^\dagger = \frac{3A^2}{4(K-H)^2} \rho_d^\dagger - \frac{3A^2}{4K^2} \rho_d^\dagger, \quad (14a)$$

$$\Delta\rho^\dagger = \frac{3A^2}{4(K+H)^2} \rho_d^\dagger - \frac{3A^2}{4K^2} \rho_d^\dagger. \quad (14b)$$

In this limit $\rho_d^{\uparrow,\downarrow}$ can be approximated by $\rho_{d0} \pm \rho_H H$ where ρ_H is just a constant reflecting the slope of the density of states with energy. Substituting in Eq. (2), one finds to lowest order in H ,

$$\frac{\Delta\rho}{\rho} = \frac{3}{4} \left[\frac{A\rho_H H}{K\rho_{d0}} \right]^2 \left[1 + \frac{4\rho_{d0}}{\rho_H K} \right]. \quad (15)$$

TABLE VI. Spin-up and spin-down anisotropic magnetoresistance $\Delta\rho$ for the doublets or triplets of an atomic d manifold in a cubic crystal field (splitting K) to second order in spin-orbit constant A , and with an exchange splitting H . Current assumed along [100].

Fermi level	$\Delta\rho^\dagger/\rho_{d0}$	$\Delta\rho^\dagger/\rho_{d0}$
Down-spin triplet	$3A^2/4(H-K)^2$	$-3A^2/4K^2$
Down-spin doublet		$(3A^2/4K^2) - 3A^2/4(H+K)$
Up-spin triplet	$-3A^2/4K^2$	$3A^2/4(H+K)^2$
Up-spin doublet	$(3A^2/4K^2) - 3A^2/4(H-K)^2$	

Thus $\Delta\rho/\rho$ goes to zero as $H \rightarrow 0$, as required physically.

The Smit spin mixing and $L_z S_z$ mechanisms, as developed by Campbell *et al.*³ and Jaoul *et al.*⁴ have, because of their apparent success in explaining experimental data, served as paradigms for understanding anisotropic magnetoresistance. Nevertheless as shown above, they suffer from the fundamental conceptual problem of the weak-ferromagnetism catastrophe. Because the new calculation with cubic anisotropy solves this problem, I advance it as a new and superior paradigm for understanding anisotropic magnetoresistance. While still very much a model calculation, it injects a feature recognized as essential by Berger⁵ and Potter,⁷ namely what could be termed a local environment or ligand field effect. They viewed this in terms of the band structure, which arises from covalent interactions between neighboring atoms. Through cubic anisotropy, I have introduced the simplest possible model of the effect of the local environment. Thus, this is a first step towards a more realistic band structure but is still simple enough to allow insight into a calculation which is already quite complicated. As shall be seen in the next section, these ideas explain experiment as well as, if not better than, any previous work.

B. Anisotropic magnetoresistance of p states

Previous theory of anisotropic magnetoresistance has focused exclusively on atomic d states. While s states, by symmetry, cannot contribute, p states can. The results of an atomic calculation, exactly analogous to that for the d states, are given in Table VII. Once again Smit-like terms give summed contributions which go as the square of

TABLE VII. Second-order eigenenergies E and resistivities ρ for the three primarily spin-down and three primarily spin-up p eigenstates of a Hamiltonian with exchange field \mathbf{H} and spin-orbit coupling \mathbf{A} ($\epsilon = A/H$). $\Delta\rho = \rho_{||} - \rho_{\perp}$ and ρ_{p0} is resistivity due to scattering off p states without spin-orbit coupling.

State	1	2	3	Sum	4	5	6	Sum
$E/H \pm \frac{1}{2}$	$-\epsilon/2 + \epsilon^2/2$	$\epsilon^2/2$	$\epsilon/2$		$\epsilon/2$	$-\epsilon^2/2$	$-\epsilon/2 - \epsilon^2/2$	
$\rho_{ }^{\uparrow}/\rho_{p0}$	$\epsilon^2/2$					$1 - \epsilon^2/2$		
$\rho_{\perp}^{\uparrow}/\rho_{p0}$		$\epsilon^2/4$			$\frac{1}{2}$		$\frac{1}{2} - \epsilon^2/4$	
$\Delta\rho^{\uparrow}/\rho_{p0}$	$\epsilon^2/2$	$-\epsilon^2/4$		$\epsilon^2/4$	$-\frac{1}{2}$	$1 - \epsilon^2/2$	$-\frac{1}{2} + \epsilon^2/4$	$-\epsilon^2/4$
$\rho_{ }^{\downarrow}/\rho_{d0}$		$1 - \epsilon^2/2$					$\epsilon^2/2$	
$\rho_{\perp}^{\downarrow}/\rho_{d0}$	$\frac{1}{2} - \epsilon^2/4$		$\frac{1}{2}$			$\epsilon^2/4$		
$\Delta\rho^{\downarrow}/\rho_{d0}$	$-\frac{1}{2} + \epsilon^2/4$	$1 - \epsilon^2/2$	$-\frac{1}{2}$	$-\epsilon^2/4$		$-\epsilon^2/4$	$\epsilon^2/2$	$\epsilon^2/4$

A/H , with signs the same as for the d states. Only the coefficient is smaller ($\frac{1}{4}$ instead of $\frac{3}{4}$). The three first-order spin-orbit-split states also give an $L_z S_z$ effect with a negative-positive-negative pattern.

A cubic ligand field does not quench the p -state anisotropic magnetoresistance because it does not split the three p states. Thus, it appears as if a weak-ferromagnetism catastrophe could occur as exchange splitting H goes to zero. In a realistic band-structure environment, however, the p states have strong dispersion. For the k vectors where p states intersect the Fermi surface, the three p states will in general be strongly split, and so one can expect terms of order $(A/K)^2$. Further discussion of the possible experimental relevance of the p -state effect appears in Sec. V B.

V. BAND STRUCTURE AND APPLICATION OF THE CUBIC-ANISOTROPY PARADIGM

In this section I give a rather qualitative discussion of the effect of band structure on anisotropic magnetoresistance. Nevertheless the concepts provide a starting point for understanding how the model results of Table VI can apply to real systems.

A. General formulas for band structure

Following Potter,⁷ one can calculate the resistivity from the square of a matrix element $V_{kk'}^{sn}$ between a propagating s state with wave vector k and a d state with wave vector k' and d -quantum number n :

$$V_{kk'}^{sn} = \int d\tau \psi_{nk'}^*(r) V(r) e^{ik \cdot r} \chi^{\pm}, \quad (16)$$

where

$$\psi_{nk'} = \sum_{l,m} e^{ik \cdot R_l} a_{nm}(k') \phi_m(r - R_l). \quad (17)$$

Here $\int d\tau$ is an integral over space. $V(r)$ is the scattering potential, which represents a difference between the potentials of the host and impurity atoms, and which is

usually assumed to be spherically symmetric; $r=0$ is the location of the impurity. χ^{\pm} is the spin state (up or down) of the propagating s state with wave function $e^{ik \cdot r}$. $\psi_{nk'}$ is the n th d -state wave function at wave vector k' , which can be decomposed as a sum over atomic d orbitals ϕ_m (including spin) and lattice sites R_l with coefficients $a_{nm}(k')$. Only d states at the Fermi surface can contribute. These can include both the host d states described above and the impurity d states which happen to also lie at the Fermi surface.

The wave functions ψ can be expanded to second order in the spin-orbit coupling. Relevant terms are

$$\psi_{nk}^{(2)} = \psi_{nk}^{(0)} \left[1 - \frac{1}{2} \sum_{n' \neq n} |A_{nn'k}|^2 \right] + \sum_{n' (\neq n)} A_{nn'k} \psi_{n'k}^{(0)}, \quad (18)$$

where

$$A_{nn'k} = \left[\int d\tau \psi_{n'k}^{(0)*} \mathbf{A} \mathbf{L} \cdot \mathbf{S} \psi_{nk}^{(0)} \right] / (E_{nk} - E_{n'k}). \quad (19)$$

If we assume that the d states are localized on atomic sites with negligible overlap between sites, then the integrals in Eqs. (16) and (19) are confined to the unperturbed atomic d states on the impurity site $R_l=0$. For example, for k parallel to the exchange field, it is easy to show that in Eq. (16) only the integral over the $3z^2 - r^2$ orbital is nonzero. This means only a single term of Eq. (17) contributes and one obtains

$$V_{kk'}^{sn} \propto a_{nm}(k') \left[1 - \frac{1}{2} \sum_{n' (\neq n)} |A_{nn'k'}|^2 \right] + \sum_{n' (\neq n)} A_{nn'k'} a_{n'm}(k'), \quad (20)$$

where m represents the $3z^2 - r^2$ d state with the same spin as the s state.

Since in general most of these coefficients are nonzero and $n \neq n'$ ranges over nine values, the square of this

quantity is, even with these approximations, quite a mess. Furthermore, to get the resistivity, a sum must be performed over all nk' combinations which correspond to d states intersecting the Fermi surface.

B. Non-VBS impurities: band averaging of $\Delta\rho/\rho$

It might be thought, in view of the complexity described above, that no meaningful prediction of $\Delta\rho/\rho$ could be made without a detailed band-structure calculation. But this very complexity suggests simplifying assumptions in certain cases which can permit a factor-of-2 comparison with experimental data.

First consider the case of the non-VBS impurities in nickel (see Table I). As pointed out in Sec. II and illustrated by Fig. 2(a), the local states of most of these impurities do not lie at the Fermi energy. Therefore, as far as scattering is concerned, the impurity site looks approximately like a *hole* in the nickel lattice. Then the relevant interpretation of $\psi_{nk'}$ of Eq. (17) is as the pure nickel band states, which remain the same, to a first approximation, whatever the impurity. Similarly, a full calculation of $\Delta\rho^\uparrow$ and $\Delta\rho^\downarrow$ from Eq. (20) will give the same answer for all non-VBS impurities. A measure of the validity of this approximation is the constancy of ρ^\uparrow in Table I for the cases Mn through Au: it works up to a factor of 2. Similarly $\Delta\rho^\uparrow/\rho^\uparrow$ varies only by a factor of 3.

Now in general for a simple transition-metal d band, the cubic splitting is usually roughly proportional to the bandwidth because it is determined by the same interactions which give rise to the band structure in the first place. Furthermore, the bandwidth of transition metals like nickel²⁰ is significantly larger than the $k=0$ cubic splitting. These facts suggest that *all* the local d states ϕ_m are coupled in to $\Delta\rho/\rho$ through Eq. (20) and its complicated $a_{n'm}(k')$ coefficients. Thus the final result will be to a rough approximation an average over the contributions of all the local d states. Like in a random-phase approximation, cross terms between the different local d states will tend to average out. This can be termed a "band-averaging" approximation.

Band averaging of $\Delta\rho/\rho$ leads to the following consequences. The doublet and triplet contributions for each spin direction in Table VI can be added together. Then the $L_z S_z$ terms $\pm 3A^2/4K^2$ cancel, and one is left with $3A^2/4(K-H)^2$ and $-3A^2/4(K+H)^2$ for $\Delta\rho^\uparrow/\rho_{d0}$ and $\Delta\rho^\downarrow/\rho_{d0}$, respectively. In other words, band averaging suppresses the $L_z S_z$ effect but leaves the pseudo-spin-mixing effect which always gives opposite signs for $\Delta\rho^\uparrow$ and $\Delta\rho^\downarrow$ in the two spin channels.

To make an estimate of the magnitude, one can average ρ just like $\Delta\rho$, and then ρ_{d0} should be of order ρ_d^\uparrow . Furthermore K can be taken as a characteristic splitting in the band structure. If there are five states at a given k vector in a band of total width 5 eV, K can be taken as roughly 1 eV. This is larger than the exchange splitting H of 0.3 eV determined from photoemission measurements.²¹ Thus K dominates H in the denominators of Table VI; so $\Delta\rho^\uparrow/\rho^\uparrow$ and $\Delta\rho^\downarrow/\rho^\downarrow$ should be positive and negative, respectively, and roughly similar in the magnitude $3A^2/4K^2$. Essentially, this is the same as the predic-

tion of Campbell *et al.*,⁴ but with K replacing their H , and so it has all the nice features of their prediction with the added advantage of avoiding the magnetic weakness catastrophe. It agrees with the average 2% magnitude of $\Delta\rho^\uparrow/\rho^\uparrow$ in Table I provided A is taken to be 0.16 eV, a factor of 4 larger than the atomic value,⁴ which is acceptable, considering uncertainties in A and K and the various coefficients.

It is also worth noting that the widely differing values of the net $\Delta\rho/\rho$ for these alloys are principally determined by the differing s scattering shown in the first column (ρ^\uparrow) of Table I. The s scattering is much more sensitive to the specific impurity than the d scattering because s states are much broader than d states, and so, the impurity s states invariably overlap the Fermi surface while impurity d states do not. Now since $\rho^\uparrow \simeq \rho_d^\uparrow$ is large, most current flows through the lower resistivity up-spin channel. Hence the first term in Eq. (2) dominates, giving

$$\Delta\rho/\rho \simeq (\Delta\rho^\uparrow/\rho^\uparrow)(\rho^\uparrow/\rho^\downarrow).$$

With roughly constant $\Delta\rho^\uparrow/\rho^\uparrow$ and ρ^\uparrow , one obtains $\Delta\rho/\rho \propto 1/\rho^\downarrow \propto 1/\rho_s$.

A further point is that the Al, Si, and Sn impurities of Table I have more p states than do the transition-metal impurities. This suggests the possibility that they could be contributing to $\Delta\rho/\rho$ according to Table VII. Since these states are even broader than the d states, one might expect Smit spin-mixing contributions, which have the same sign as for the d states and thus should enhance the $\Delta\rho$'s. There is indeed some evidence for such an enhancement if one compares $\Delta\rho^\uparrow$ for transition-metal and non-transition-metal groups in Table I. However $\Delta\rho^\downarrow$ does not show an effect. Of course, one complication is that the p states are so much less localized than the d states that they themselves may contribute to conduction. Furthermore they are likely to be less exchange split than the d states. A more precise theory of such an effect has not been developed.

C. Weak ferromagnetism in Ni-Fe

For more concentrated alloys, the considerations of the last section change. For the specific case of iron in nickel, as mentioned earlier, the Fermi level lies in a down-spin predominantly iron d band above 20% iron, and above 50%, weak ferromagnetism appears [Fig. 2(b)]. Now the scattering is due to iron d states rather than nickel holes. To predict $\Delta\rho/\rho$ one must consider that the iron band is relatively broad, and therefore, using the same arguments as in the previous section, an average over terms like those in Table VI should be expected. Furthermore, to account for weak ferromagnetism, contributions from both up- and down-spin d -state scattering should be included. Therefore the relevant formula is Eq. (9), with γ taken to be approximately proportional to $(A/K)^2$, and again K should be interpreted as proportional to the iron bandwidth.

Crucial now are two effects characteristic of the concentrated alloy case¹² and differing from the dilute impurity limit discussed before. First is the fact that the iron bandwidth changes as a function of composition. To a first approximation, this change is linear in the concen-

trated region, though in the dilute region it breaks away to a constant value determined by iron-nickel rather than iron-iron interactions. Therefore γ in Eq. (9) will change as $g/(1-x_{\text{Fe}})^2$, where g is a constant. Second is the fact that in the concentrated alloy limit, as first pointed out by Mott,²² d scattering is roughly proportional to the d density of states, which is in turn proportional to the d part of the known¹⁵ electronic specific heat γ_H :

$$\rho_d^\dagger + \rho_d^\dagger = (\gamma_H - \gamma_s)c. \quad (21)$$

Here c is a constant proportional to the square of a scattering matrix element, assumed not to be composition dependent, and γ_s is the sp-electron specific heat of approximately 1 mJ/mol K².

These results, coupled with known¹⁵ data on the total resistivity ρ :

$$\rho^{-1} = (\rho_s + \rho_d^\dagger)^{-1} + (\rho_s + \rho_d^\dagger)^{-1}, \quad (22)$$

allow calculation of $\Delta\rho/\rho$ provided ρ_s is known as a function of concentration and the constants c and g are determined. The Nordheim rule and a rough fit to ρ in the nickel-rich end where ρ_s dominates, gives $\rho_s \simeq 22x(1-x)$. c is determined in terms of g by normalizing $\Delta\rho/\rho$ at $x_{\text{Ni}}=0.7$.

Figure 1 shows as solid lines the resulting concentration dependence for two choices of g , corresponding to γ values of 0.005 and 0.01 at $x_{\text{Ni}}=0.7$. The dependence is seen to be insensitive to the choice of γ . The results are in excellent agreement with experimental data, the overestimate at 0.75 arising from the rollover to a more constant bandwidth in the dilute iron limit as discussed earlier. On the other hand, if one ignores the ρ_d^\dagger term in Eq. (9), which comes from magnetic weakness, and if one neglects the bandwidth concentration dependence, one obtains the dotted curves in Fig. 1 for the two choices of γ . While still showing a decrease, which comes principally from the increasing ρ_s , these earlier predictions¹² are clearly inadequate to account for the sharpness of the falloff in $\Delta\rho/\rho$ with increasing x_{Fe} in the weak-ferromagnetic region.

The predicted ρ_d^\dagger corresponding to the full calculation of Fig. 1 is roughly constant at 60–70 $\mu\Omega$ cm for $\gamma=0.01$, while ρ_d^\dagger increases from essentially zero above $x_{\text{Ni}}=0.55$ to 10 $\mu\Omega$ cm at $x_{\text{Ni}}=0.45$. It is not surprising that these results differ from those of Muth and Christoph,¹¹ and of Campbell,⁹ who deduced the subband resistivities from a very different and most likely incorrect choice of γ 's as discussed in Sec. II. In summary, the Fe-Ni Invar example illustrates again the importance of accounting for band structure in the treatment of anisotropic magnetoresistance.

D. VBS impurities in nickel

The treatment for VBS impurities in nickel must again differ from the previous cases because of differences in the band structure. In these cases the VBS levels at the up-spin Fermi level are expected to be sharp. For example, the width of the $3d$ levels is less than 0.1 eV; it increases to $\simeq 0.5$ eV for the $5d$ levels.⁴ If in the cubic anisotropy paradigm K remains proportional to the bandwidth, it will also be small. Then the $\pm 3A^2/4K^2$ terms

for the up-spin doublet and triplet in Table VI will be large compared to the $\pm 3A^2/4(H \pm K)^2$ terms. Here the situation is reversed from the non-VBS alloys, where the relevant limit was K greater than H . As already pointed out by Jaoul *et al.*,⁴ A also increases from the $3d$ to $4d$ to $5d$ series, and contributions of order $(A/W)^2$ or $(A/K)^2$ are in the right range to explain the size of $\Delta\rho^\dagger/\rho^\dagger$ in Table I.

But now interesting differences appear with the previous interpretation of Jaoul *et al.* States of doublet character will tend to lie highest because their orbitals are non-bonding in the fcc environment. This tendency can also be seen in the $k=0$ splittings of fcc transition-metal band structures.²⁰ Consider now a series of $3d$ impurities, whose d states rise in energy moving to the left in the Periodic Table. Thus the first states to intercept the Fermi surface will be doubletlike states. The triplet states, lying lower in energy, will tend to hybridize with the nickel host band. Interesting evidence supporting this hypothesis comes from recent impurity calculations of Dederichs *et al.*²³ They show a large weight of impurity states lying opposite the host d band, while only approximately two states per atom lie in the sharp VBS peak near the Fermi energy (e.g., see results for Cr, V, and Ti impurities in Fig. 5 of Ref. 23).

If the sharp VBS's are actually primarily of up-spin doublet character, they should give a predominantly positive contribution according to Table VI. The up-spin triplet states presumably then lie primarily in the broad band opposite the host nickel states, and their negative contribution should not appear. This accords nicely with experiment on the $3d$ and $4d$ VBS alloys which show a roughly constant positive value for $\Delta\rho^\dagger/\rho^\dagger$ as one shifts across the Periodic Table (see Table I). By contrast Jaoul *et al.*⁴ predicted a negative-positive-negative pattern, for which there is no experimental evidence in these series.

The fact that the up-spin doublet terms are predominantly positive for the $3d$ and $4d$ series does not prevent the net $\Delta\rho/\rho$ from being negative, as found experimentally for many of these systems. The negative values can be traced to the additional spin-mixing contributions from primarily down-spin nickel hole states. Since the d scattering of the virtual bound states is so strong, ρ^\dagger exceeds ρ^\dagger , and most current flows through the down-spin channel. Thus the negative $\Delta\rho^\dagger$ contribution of the nickel holes is weighted most heavily in Eq. (2).

One must still ask why positive spin-mixing contributions of order $3A^2/4H^2$ are not observed in $\Delta\rho^\dagger/\rho^\dagger$. These should be at least 2% for the $3d$ VBS series and larger for the $4d$ and $5d$ series. Table VI suggests a possible answer: Such terms are absent for the up-spin doublet and only present in the up-spin triplet. In other words, Eq. (11) rather than (13) applies, with 3β given by the up-spin doublet entry of Table VI. This answer is not entirely satisfactory, however, because the absence of these terms is surely a special result of the [100] orientations for the currents in the calculation of Table VI. The experimental measurements, on the other hand, are usually done on polycrystalline samples with random orientations. A more complete answer on this point awaits a generalization of Table VI to arbitrary orientations.

A further question concerns the appearance of negative $\Delta\rho^{\uparrow}$ for Ir in the $5d$ series, which seems to contradict the interpretation given above. Table VI suggests a natural explanation. Since the bandwidth and therefore the effective K of the $5d$ series is larger than for the $3d$ and $4d$ series, K may now approach or exceed H , and therefore the negative $3A^2/4(H-K)^2$ term for the up-spin doublet in Table VI can dominate. To explain why Pt or Re are still positive, one must argue that the prominence of this negative term is very sensitive to the precise values of H and K .

The most serious problem with this interpretation is that if indeed the VBS density of states consists of a doublet while the triplet impurity states are spread at lower energy opposite the nickel d states, then the size of the cubic splitting K is ambiguous: Is it proportional to the width of the sharp VBS feature, as assumed above, or is it related to the much larger energy difference between the centers of the nickel and doublet VBS bands? If the latter, then K would be much larger than H and the interpretation would fail. The cubic-anisotropy paradigm, of course, cannot in itself clarify this more detailed band-structure effect. So pending a more detailed treatment, the above interpretation must be viewed as a hypothesis which nevertheless accounts for the experimental trends better than previous work.

VI. CONCLUSIONS

This has been a rather elaborate treatment of a wide range of experimental data and theory on anisotropic magnetoresistance. Concepts have been synthesized from

a number of authors: the spin-mixing effect of Smit² and Campbell *et al.*,³ the $L_z S_z$ effect of Jaoul *et al.*,⁴ the role of band splittings by Berger⁵ and Potter,⁷ and the phenomenological generalization of Muth and Christoph.¹¹ Added to this group is the notion of the weak-ferromagnetism catastrophe, the role of p states, the band averaging over local d states, and, most important, the effect of cubic anisotropy, which had never been presented before with a correct treatment of symmetry, matrix elements, and second-order normalization effects.

The qualitative success in understanding so many different systems based on ferromagnetic nickel shows the usefulness of the cubic-anisotropy calculation as a new paradigm for understanding anisotropic magnetoresistance. Clearly each system must be considered on its own merits, with different Muth-Christoph phenomenological parameters applying in each case. This has led to new phenomenological formulas, like Eqs. (6), (9), and (13), for the special cases of (1) non-VBS strong, (2) weak, and (3) VBS alloys. This work clearly calls for a more detailed band-structure treatment of anisotropic magnetoresistance. Nevertheless it gives confidence in a framework which is apparently taking the most relevant phenomena into account.

ACKNOWLEDGMENTS

The author thanks I. A. Campbell and L. Berger for key discussions on the anisotropic magnetoresistance theory, A. R. Williams and J. Tersoff for essential input on the possibility of doublet structure in the virtual bound states, and T. R. McGuire and P. Freitas for insights into the experimental data.

-
- ¹T. R. McGuire and R. I. Potter, *IEEE Trans. Magn.* **11**, 1018 (1975).
²J. Smit, *Physica (Utrecht)* **17**, 612 (1951).
³I. A. Campbell, A. Fert, and O. Jaoul, *J. Phys. C* **3**, S95 (1970).
⁴O. Jaoul, I. A. Campbell, and A. Fert, *J. Magn. Magn. Mater.* **5**, 23 (1977). Note that in their Fig. 9, the phase is offset by $\pi/2$.
⁵L. Berger, *Physica (Utrecht)* **30**, 1141 (1964).
⁶L. Berger and S. A. Friedberg, *Phys. Rev.* **165**, 670 (1968).
⁷R. I. Potter, *Phys. Rev. B* **10**, 4626 (1974). Table II of the present paper corrects Table II of this reference.
⁸J. W. F. Dorleijn, *Philips Res. Rep.* **31**, 287 (1976).
⁹I. A. Campbell, *J. Phys. F* **4**, L181 (1974).
¹⁰N. F. Mott, *Proc. R. Soc. London, Ser. A* **153**, 699 (1936).
¹¹P. Muth and V. Christoph, *J. Phys. F* **11**, 2119 (1981).
¹²A. P. Malozemoff, *Phys. Rev. B* **32**, 6080 (1985).
¹³A. Fert and I. A. Campbell, *Phys. Rev. Lett.* **21**, 1190 (1968).
¹⁴L. Berger, *Magnetism and Magnetic Materials—1976 (Joint MMM-Intermag Conference, Pittsburgh)*, Partial Proceedings

- of the First Joint *MMM-Intermag Conference*, AIP Conf. Proc. **34**, edited by J. J. Becker and G. H. Lander (AIP, New York, 1976), p. 355.
¹⁵Y. Nakamura, in *Physics and Applications of Invar Alloys*, edited by H. Saito (Maruzen, Tokyo, 1978), p. 123.
¹⁶J. Friedel, in *Metallic Solid Solutions*, edited by J. Friedel and A. Guinier (Benjamin, New York, 1963), p. XIX-1.
¹⁷L. I. Schiff, *Quantum Mechanics* (McGraw-Hill, New York, 1955), p. 154.
¹⁸V. A. Marsocci, *Phys. Rev.* **137**, A1842 (1965).
¹⁹G. Thomas, V. A. Marsocci, and P. K. Lin, *Physica (Utrecht)* **45**, 407 (1969).
²⁰V. Moruzzi, J. F. Janak, and A. R. Williams, *Calculated Electronic Properties of Metals* (Pergamon, New York, 1978).
²¹D. E. Eastman, F. J. Himpsel, and J. A. Knapp, *Phys. Rev. Lett.* **40**, 1514 (1978).
²²N. F. Mott, *Philos. Mag.* **26**, 1249 (1972).
²³P. H. Dederichs, R. Zeller, H. Akai, S. Bluegel, and A. Oswald, *Philos. Mag. B* **51**, 137 (1985).